Structural Engineering and Mechanics, Vol. 5, No. 2 (1997) 177-191
DOI: http://dx.doi.org/10.12989/sem.1997.5.2.177

Fluid viscous device modelling by fractional derivatives

V. Gusella† and G. Terenzi‡

Institute of Energetics, Faculty of Engineering, University of Perugia, Strada S. Lucia Canetola, 06125 Perugia, Italy

Abstract. In the paper, a fractional derivative Kelvin-Voigt model describing the dynamic behavior of a special class of fluid viscous dampers, is presented. First of all, in order to verify their mechanical properties, two devices were tested the former behaving as a pure damper (*PD* device), whereas the latter as an elastic-damping device (*ED* device). For both, quasi-static and dynamic tests were carried out under imposed displacement control.

Secondarily, in order to describe their cyclical behavior, a model composed by an elastic and a damping element connected in parallel was defined. The elastic force was assumed as a linear function of the displacement whereas the damping one was expressed by a fractional derivative of the displacement. By setting an appropriate numerical algorithm, the model parameters (fractional derivative order, damping coefficient and elastic stiffness) were identified by experimental results.

The estimated values allowed to outline the main parameter properties on which depend both the elastic as well as the damping behavior of the considered devices.

Key words: fractional derivative Kelvin-Voigt model; pure damper (*PD* device); elastic damper (*ED* device); fractional oscillator.

1. Introduction

The calamity which occurred in Japan in 1994 also recently evidenced the importance of aseismic design. Every year, earthquakes cause significant life loss and structural damage in many countries of the World. In attempts to mitigate the effects of seismic actions on buildings, bridges and potentially vulnerable contents, many aseismic construction designs and technologies have been developed.

In this context, seismic isolation is a relatively recent and evolving technology which consists essentially of installing mechanisms capable of decoupling the ground motion from the structural one (Buckle and Mayes 1990, Korenev and Reznikov 1993, Kelly 1993, Skinner, Robinson and McVerry 1993). This decoupling is achieved by increasing the flexibility of the system, along with providing appropriate damping.

The use of fluid viscous devices for seismic isolation of buildings and bridges represents a very interesting new vibration control strategy. Operating on the principle of fluid flow through orifices, these devices consist of a moving piston in a steel cylinder filled with polymeric material, obtained by applying special chemical processes to silicon and other components (e.g., hydrocarbons).

First used in the 75 mm French artillery rifle of 1897, after the Second World War they

† Associate Professor
‡ Ph.D.-Post Doctoral Student

were introduced as shock dampers and vibration isolation systems in mechanical applications and civil realizations such as aerospace and railway hardware. Since only ten years ago they have been proposed for seismic isolation of buildings and bridges. Regarding this, in 1985 Huffmann (Huffman 1985) presented a system of helical steel springs and viscous dampers. Soon after in 1992, Makris and Constantinou (Makris and Constantinou 1990) analyzed a kind of viscous dampers produced in the United States characterized by a hollow piston movable in all directions.

The devices considered in this paper represent a special class of fluid viscous dampers. Their piston element is rod-shaped, its head being of greater section, and without holes. The dimension design of every element and the chemical composition of the silicon material determine the mechanical behavior of the device which can be a pure damper, an elastic-damping device, or an elastic system.

In order to efficiently use these systems for seismic applications, an appropriate analytical model needs to be defined which interprets the dynamic behavior; this problem hasn't been solved yet.

In literature, two main models representing the polymeric materials' rheological behavior are proposed: the non-linear Kelvin-Voigt model, and the fractional-derivative Maxwell model. The former is characterized by a prestressed spring, and a dashpot to which corresponds a viscous law: $c\,sgn(v)|v(t)|^{\alpha}$, where "c" is a constant coefficient, "v" is the velocity, and "α" is an exponent less than one (Terenzi 1994); the second, proposed by Makris and Constantinou (Makris and Constantinou 1990, Makris 1992), simulates the force-displacement behavior of U.S. fluid viscous dampers by using fractional derivatives (or "generalized derivatives", Nashif 1985).

In this paper, two types of fluid viscous devices produced in France are analyzed. On the basis of experimental survey results, a *fractional-derivative Kelvin-Voigt model* is proposed. Introduced in a step-by-step integration procedure, it allows to evaluate the dynamic response of structural systems isolated by these kinds of devices.

2. Experimental tests

In order to define the mechanical properties of fluid viscous dampers, two devices the first of which behaves as a pure damper (*PD* device), whereas the second is an elastic damper (*ED* device), were tested.

The different ratio between the rod and the head piston, and the internal section of the outer casing is one of the more important parameters characterizing the mechanical behavior of the system. For example, in the case of the *PD* device, the piston goes through the cylinder filled with the silicone-based elastomeric material. Moreover, the difference between the section of the piston head and the internal section of the cylinder is very small. Thanks to these geometrical properties, the system (Fig. 1) behaves like a pure damper. On the other hand, in the case of the *ED* device (Fig. 2) with head section smaller than the one of the pure damper, the piston doesn't go through the outer casing, giving to the system a damping behavior as well as an elastic one.

For both devices, quasi-static and dynamic tests were carried out under imposed displacement control. Sinusoidal displacement time histories were applied in the tests, the characteristics of which (frequency, displacement and velocity amplitude, number of cycles) are presented in Table.

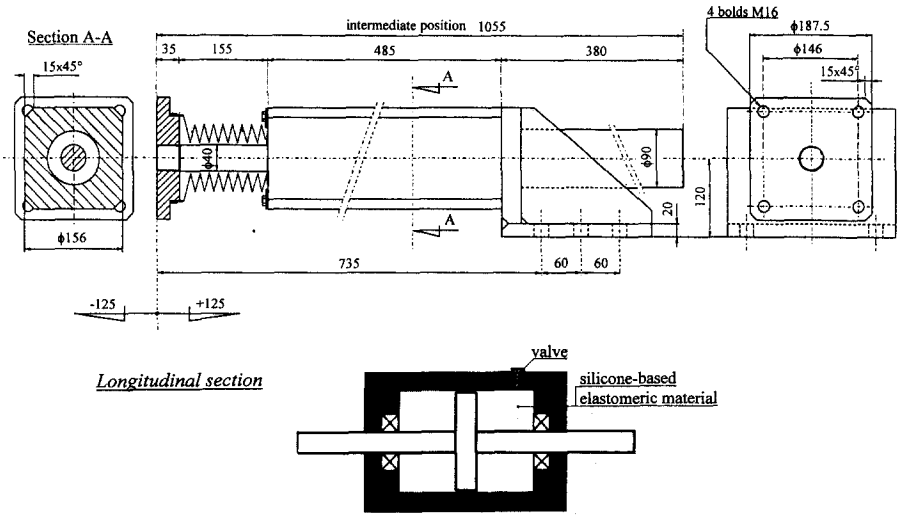

Fig. 1 Geometrical representation of the *PD* device and longitudinal section scheme.

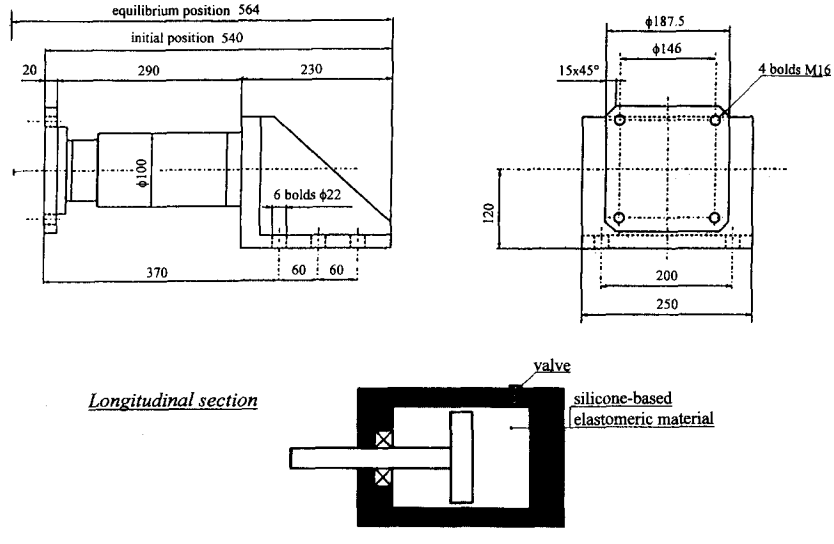

Fig. 2 Geometrical representation of the *ED* device and longitudinal section scheme.

1, with reference to the *PD* device, and in Table 2, with reference to the *ED* system. In the case of the first damper, thermal changes ΔT also occurring throughout the tests were surveyed. On the whole, low ΔTs were observed (i.e., -Table 1- in the 7*PD* test, characterized by 100 cycles, a ΔT equal to 15.3℃ was evaluated). It can be noted that the tests on the *PD* device were started from the median position with respect to the cylinder, corresponding to the static equilibrium position without external forces. The median position was also imposed at the beginning of the tests of the elastic damper, even though for this system designed as a single-acting device, the static equilibrium position is the one characterized by the whole piston rod out of the casing. This intermediate position was assigned in order to make the device operate in a double-acting fashion by initially imposing a force equal to the internal pressure of the silicon fluid multiplied

Table 1 Main characteristics of experimental tests carried out on the *PD* device

Test name	Frequency (Hz)	Amplitude (mm)	Velocity (mm/s)	Time duration (s)	Number cycles	ΔT (°C)
1*PD*	0.1	16.2	10.2	50	5	
2*PD*	0.1	30.2	19	50	5	
3*PD*	0.1	58.3	36.6	40	4	
4*PD*	0.3	30.5	57.4	34	10	0.5
5*PD*	0.3	57.7	108.8	28	8.5	0.6
6*PD*	0.3	91.6	172.7	27	8	2
7*PD*	0.5	17.8	55.9	200	100	15.3
8*PD*	0.5	33.3	104.5	100	50	1.6
9*PD*	0.5	33.5	105.2	100	50	1.2
10*PD*	1	10.4	65.3	5	5	

Table 2 Main characteristics of experimental tests carried out on the *ED* device

Test name	Frequency (Hz)	Amplitude (mm)	Velocity (mm/s)	Time duration (s)
1*ED*	0.1	17.5	11	90
2*ED*	0.1	22.5	14.3	90
3*ED*	0.3	17.5	33	34
4*ED*	0.3	20.0	37.6	34
5*ED*	0.5	17.5	54.9	20
6*ED*	0.75	11.0	51.8	14
7*ED*	1.0	16.5	103.4	10
8*ED*	2.0	13.8	17	5
9*ED*	3.0	10.7	197.6	3

by the area of the rod section. Generally, the experimental results showed the elastic-damping behavior and the thermal stability of the devices. With respect to the pure damper in Figs. 3-4, some displacement and reaction force time histories are presented whereas Fig. 5 shows the relative hysteretical loops. This last figure points out the high damping stability.

With respect to the *ED* device in Figs. 6-7, some displacement and reaction force time histories are presented whereas Fig. 8 shows the relative hysteretical loops. In this last figure, the stability of the mechanical behavior was generally confirmed also for the elastic damper. The cycle shape is that of a damping parallelogram rotated in the plane *F-u* (reaction force-displacement) with respect to the elastic stiffness. From a physical point of view, it can be noted that when quasi-static inputs are imposed to the *ED* device, a force equal to the pressure of the silicon fluid multiplied by the area of the rod has to be initially applied in order to move the piston. On the other hand, when dynamic actions are imposed to the system the piston can move only if the external force is equal to the sum of a damping force and the previously mentioned elastic one. This last consideration especially suggested the identification of a Kelvin-Voigt model, for which the elastic element is connected in parallel to the damping element.

3. Fractional oscillator model

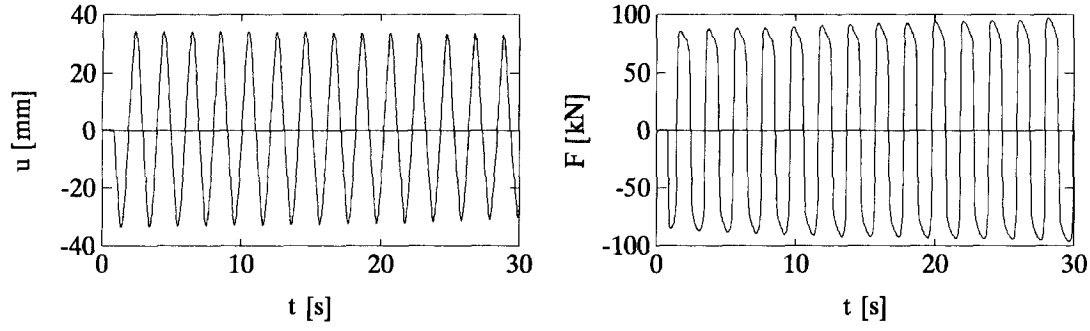

(a) time history displacement (b) time history reaction force

Fig. 3 9*DP* test results.

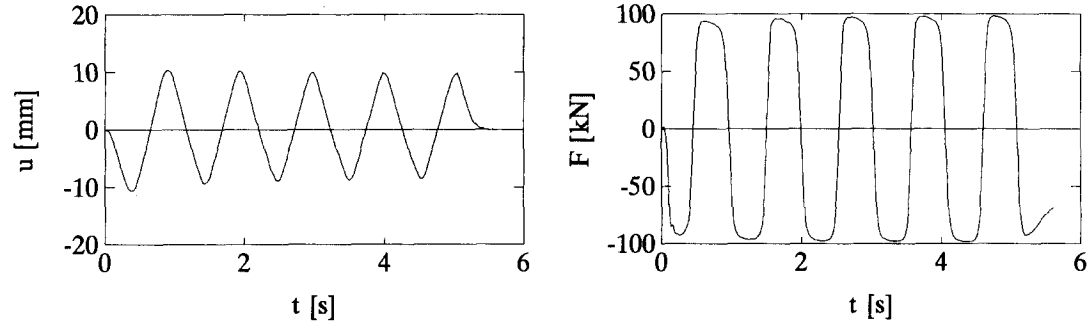

(a) time history displacement (b) time history reaction force

Fig. 4 10*DP* test results.

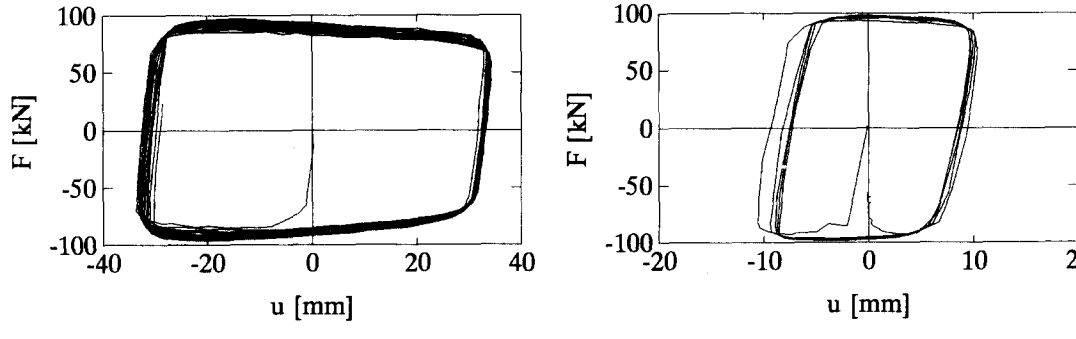

(a) 9*DP* test (b) 10*DP* test.

Fig. 5 Hysteretical loops.

Before presenting the model proposed to interpret the fluid viscous device mechanical behavior, one may observe that the macroscopic approach of rheology works in terms of state equations. Depending on the effect of external excitation, these equations describe the material behavior to some degree of approximation. Several of the most important representations of state equations are known as: the standard linear model, the generalized standard, and the generalized derivatives model (Nashif 1985).

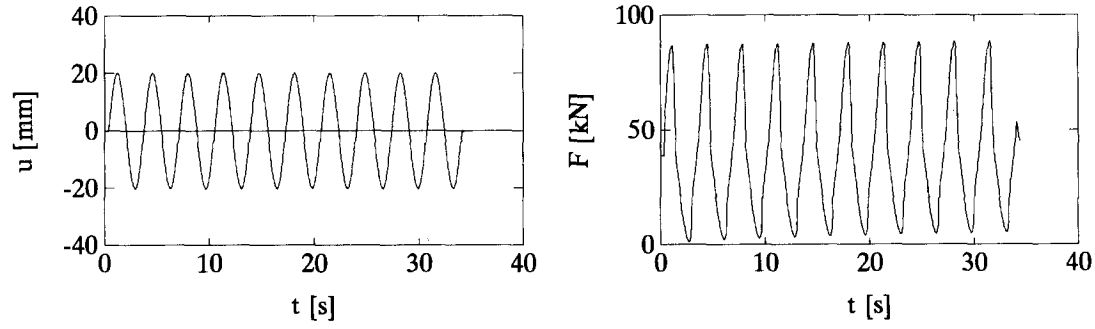

(a) time history displacement (b) time history reaction force

Fig. 6 4*ED* test results.

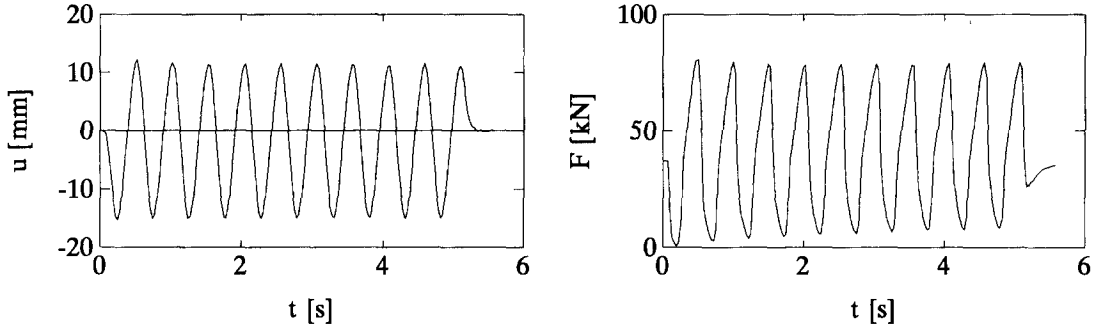

(a) time history displacement (b) time history reaction force

Fig. 7 8*ED* test results.

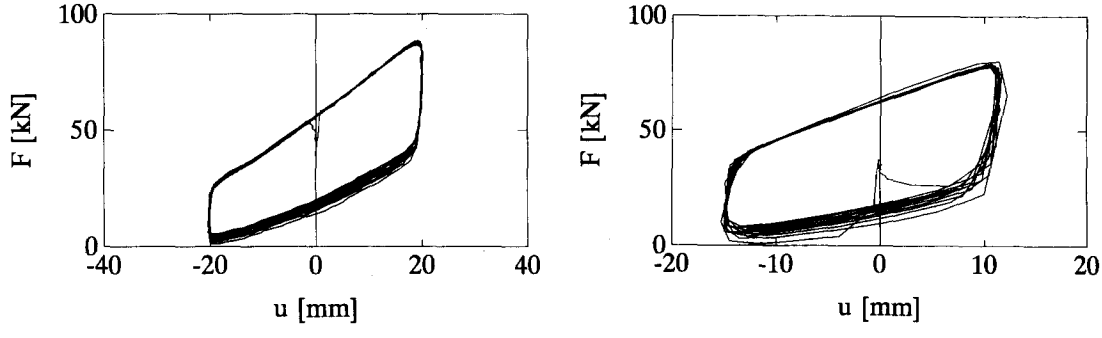

(a) 4*ED* test (b) 8*ED* test

Fig. 8 Hysteretical loops.

"Standard linear model" is the one which gives the following relationship between stress σ and strain ε:

$$\sigma+\alpha\frac{d\sigma}{dt}=E\varepsilon+\beta E\frac{d\varepsilon}{dt} \tag{1}$$

where α and β are two constants. This equation represents a more complex relationship than

either Hooke's law or the simple dashpot-spring combination, for which:

$$\sigma=E\varepsilon+E\beta\frac{d\varepsilon}{dt} \tag{2}$$

Relations (1) and (2) represent the real behavior of polymeric materials with difficulty. In fact, by applying harmonically varying stress and strain, of the $\sigma=\sigma_0 e^{i\omega t}$ and $\varepsilon=\varepsilon_0 e^{i\omega t}$ type, these formulations are related by the following expressions:

$$\sigma_0=(E'(\omega)+iE''(\omega))\,\varepsilon_0 \tag{3}$$

where:

$E'(\omega)$=real part of Young's modulus,
$E''(\omega)$=imaginary or quadrature part of Young's modulus.

In the model, the E' and E'' variation with the circular frequency ω is more rapid than the experimentally observed one.

A better interpretation of this effect may be obtained by applying the generalized standard model for which the σ-ε relationship can be written as:

$$\sigma+\sum_{n=1}^{\infty}\alpha_n\frac{d^n\sigma}{dt^n}=E\varepsilon+E\sum_{n=1}^{\infty}\beta_n\frac{d^n\varepsilon}{dt^n} \tag{4}$$

where α_n and β_n are the n-th constants. The expression corresponding in this case to Eq. (3) contains two functions $E'(\omega)$ and $E''(\omega)$ much more complicated than those characterizing the former model. As shown by Eq. (4), the generalized standard model reduces the limitations deriving from the standard linear one by introducing additional derivatives of σ and ε. Nevertheless, it should be noted that generally, a considerable number of terms is needed to appropriately represent the mechanical behavior of a real material over a wide frequency range.

In order to reduce the terms required, the derivatives of the integer order presented in Eq. (4) can be replaced by fractional derivatives, that is:

$$\sigma+\sum_{n=1}^{\infty}a_n\frac{d^{\alpha_n}\sigma}{dt^{\alpha_n}}=E\varepsilon+E\sum_{n=1}^{\infty}b_n\frac{d^{\beta_n}\varepsilon}{dt^{\beta_n}} \tag{5}$$

where:

a_n, b_n=constants,
$0<\alpha_n<1$, $0<\beta_n<1$=fractional derivative orders.

If the parameters are well chosen, more than one value of a_n and b_n is not often needed. Eq. (5) represents the "generalized derivatives model", generally proposed to interpret the rheological behavior of polymeric materials.

With respect to the tested devices, starting from the experimental results, it was already noted that the presence of an elastic component determines almost only the rotation of the damping cycle in the plane *F-u*. This fact outlines the superimposition of the elastic and damping effects in order to define the global mechanical behavior of the system. Moreover, the mean rotation angle - the value of which is the same for every test - pointed out the independence from frequency of the elastic force characterizing the considered device. Due to the silicon fluid which resists to the coming piston, this behavior can be interpreted as a parabolic function of the displacement such as the one representing the relation existing between the pressure and the

volume variations of the material. Nevertheless, based on the fact that (Terenzi 1994) considerable differences were not noted in the dynamic response deriving from a parabolic and a linear elastic model, in the present context the elastic force was expressed as:

$$F_e[u(t)]=ku(t) \tag{6}$$

where k is the elastic stiffness.

Moreover, by considering the damping effect essentially due to the difficulty of the silicon fluid to flow from one side of the casing to the other, and therefore to the shear stressed material moving into the annular space around the piston head for which the stress-strain (τ-γ) relationship is:

$$\tau(t)=G_0\gamma(t)+c_1G_0D^q[\gamma(t)] \tag{7}$$

where G_0 is the shear modulus, c_1 is a damping coefficient, and $q(0\leq q\leq 1)$ is the derivative order (known as the memory parameter), the dynamic behavior of the system can be written as:

$$m\ddot{u}(t)+cD^q[u(t)]+F_e[u(t)]=F(t) \tag{8}$$

Eq. (8), where m and c represents the moving elements mass, and the damping coefficient respectively, defines the dynamic equation of a "Kelvin-Voigt fractional oscillator model". With reference to the tested devices, the coefficient characterizing the relative mechanical behavior models were identified based on the experimental results.

4. The fractional differintegral

The adopted following notation:

$$\frac{d^nf}{dx^n} \tag{9}$$

and,

$$\frac{d^{-n}f}{d[x]^{-n}}=\int_0^x dx_{n-1}\int_0^{x_n-1}dx_{n-2}\cdots\int_0^{x_2}dx_i\int_0^{x_1}f(x_0)\,dx_0 \tag{10}$$

indicate the n-th derivative of a function f with respect to x when n is a non negative integer, and the multiple integration with zero lower limit, respectively.

Based on the identity:

$$\int_a^x f(y)\,dy=\int_0^{x-a}f(y+a)\,dy \tag{11}$$

we define:

$$\frac{d^{-n}f}{d[x-a]^{-n}}=\int_a^x dx_{n-1}\int_a^{x_n-1}dx_{n-2}\cdots\int_a^{x_2}dx_1\int_a^{x_1}f(x_0)\,dx_0 \tag{12}$$

in order to extend the symbolism to lower limits other than zero.

The ordinary definition of derivative in terms of backward difference, suggests the following general formula for n-th derivative:

$$\frac{d^n f}{dx^n} = \lim_{\delta x \to 0} \left\{ [\delta x]^{-n} \sum_{j=0}^{n} [-]^j \binom{n}{j} f(x - j\delta x) \right\} \tag{13}$$

By considering the Riemann integral we obtain:

$$\frac{d^{-n} f}{d[x-a]^{-n}} = \lim_{\delta_N x \to 0} \left\{ [\delta_N x]^n \sum_{j=0}^{N-1} \binom{j+n-1}{j} f(x - j\delta_N x) \right\} =$$

$$= \lim_{N \to \infty} \left\{ \left[\frac{x-a}{N} \right]^n \sum_{j=0}^{N-1} \binom{j+n-1}{j} f\left(x - j \left[\frac{x-a}{N} \right] \right) \right\} \tag{14}$$

where $\delta_N x = [x-a]/N$, $N = 1, 2, \cdots$

By embracing the notions of difference quotients and Riemann sums in a single Relation, Eq. (13) can be modified as:

$$\frac{d^n f}{dx^n} = \lim_{\delta_N x \to 0} \left\{ [\delta_N x]^{-n} \sum_{j=0}^{n} [-]^j \binom{n}{j} f(x - j\delta_N x) \right\} \tag{15'}$$

and, since $\binom{n}{j} = 0$ if $j > n$ when n is integer:

$$\frac{d^n f}{dx^n} = \lim_{N \to \infty} \left\{ \left[\frac{x-a}{N} \right]^{-n} \sum_{j=0}^{N-1} [-]^j \binom{n}{j} f\left(x - j \left[\frac{x-a}{N} \right] \right) \right\} \tag{15''}$$

where it was supposed that δx tends to zero through discrete values and $a < x$ plays a role like lower limits. The comparison between Eq. (15″) and Eq. (14), permits to introduce the equation:

$$\frac{d^q f}{d[x-a]^q} = \lim_{N \to \infty} \left\{ \frac{\left[\frac{x-a}{N} \right]^n}{\Gamma(-q)} \sum_{j=0}^{N-1} \frac{\Gamma(j-q)}{\Gamma(j+1)} f\left(x - j \left[\frac{x-a}{N} \right] \right) \right\} \tag{16}$$

where:

q = integer of either sign,

Γ = Gamma function.

Based on the Grüwald-Post approach, Eq. (16) can be considered as the fundamental definition of *differintegral* of order q *arbitrary*. This definition involves the fewest restrictions on the function to which it applies, and avoids explicit use of the notions of ordinary derivative and integral involving only evaluations of the function itself.

In order to describe the numerical algorithm utilized to integrate the fractional oscillator, a different definition was needed to be introduced. Starting from Leibniz's theorem for differentiating an integral:

$$\frac{d^{-1} f}{[d(x-a)]^{-1}} = \int_a^x f(y)\, dy = \frac{1}{n!} \frac{d^n}{dx^n} \int_a^x [x-y]^n f(y)\, dy \tag{17}$$

the $[n-1]$-fold integration produced Cauchy's formula for repeated integration:

$$\frac{d^{-n} f}{[d(x-a)]^{-n}} = \int_a^x dx_{n-1} \int_a^{x_{n-1}} \cdots \int_a^{x_1} f(x_0)\, dx_0 = \frac{1}{(n-1)!} \int_a^x [x-y]^{n-1} f(y)\, dy \tag{18}$$

Eq. (18) permits to define an integral of fractional order via an integral transformation called the "Riemann Liouville integral":

$$\left[\frac{d^q f}{[d(x-a)]^q}\right]_{R-L} = \frac{1}{\Gamma(-q)}\int_a^x [x-y]^{-q-1} f(y)\,dy \quad q<0 \tag{19}$$

Eq. (19) is identical to Eq. (16) for $q<0$ (fractional integral) (Oldham and Spanier 1970) so that the symbol $[]_{R-L}$ can be dropped. For $q\geq 0$ (fractional derivative) it should be utilized:

$$\frac{d^q f}{d[x-a]^q} = \sum_{k=0}^{n-1} \frac{[x-a]^{k-q} f^{(k)}(a)}{\Gamma(k-q+1)} + \frac{1}{\Gamma(n-q)}\int_a^x \frac{f^{(n)}(y)\,dy}{[x-y]^{q-n+1}} \quad n>q \tag{20}$$

which yields results identical to those given by Eq. (16), also.

5. Integration numerical algorithm

In literature many identification criteria of the parameters characterizing the fractional model have been proposed. Among these, it can be mentioned the one presented by Enelund and Olsson (1995) which is based on time domain expressions for the relaxation modulus (Bird, Armstrong and Hassager 1987). In the present research the parameters of the proposed fractional oscillator model were alternatively identified by employing the following procedure for both tested devices. An integration numerical algorithm, similar to the one utilized by Koh and Kelly (1990) to analyze the mechanical behavior of elastomeric isolation systems, was set-up. It allows to calculate the fractional derivative of the displacement by applying the $L1$-algorithm previously proposed by Oldham and Spanier (1974). In order to obtain a procedure valid for $0\leq q<1$, Eq. (20) can be utilized by assuming $a=0$ and $n=1$:

$$\begin{aligned}\frac{d^q f}{dx^q} &= \frac{x^{-q} f(0)}{\Gamma(1-q)} + \frac{1}{\Gamma(1-q)}\int_0^x \left[\frac{df}{dy}(y)\right]\frac{dy}{[x-y]^q} \\ &= \frac{1}{\Gamma(1-q)}\left\{\frac{f(0)}{x^q} + \sum_{j=0}^{N-1}\int_{jx/N}^{(jx+x)/N}\left[\frac{df}{dy}(x-y)\frac{dy}{y^q}\right]\right\}\end{aligned} \tag{21}$$

As regards the integral in Eq. (21), the $L1$-algorithm operates the following approximation:

$$\begin{aligned}\int_{jx/N}^{(jx+x)/N}\left[\frac{df}{dy}(x-y)\frac{dy}{y^q}\right] &\approx \frac{f\left(x-\frac{jx}{N}\right)-f\left(x-\frac{x}{N}-\frac{jx}{N}\right)}{\frac{x}{N}}\int_{jx/N}^{(jx+x)/N}\frac{dy}{y^q} \\ &= \frac{x^{-q}N^q}{1-q}[f_j-f_{j+1}][(j+1)^{1-q}-j^{1-q}]\end{aligned} \tag{22}$$

consequently obtaining for q-order fractional derivative the following formulation:

$$\frac{d^q f}{dx^q} = \frac{x^{-q}N^q}{\Gamma(2-q)}\left[\frac{(1-q)f_N}{N^q} + \sum_{j=0}^{N-1}[f_j-f_{j+1}][(j+1)^{1-q}-j^{1-q}]\right] \tag{23}$$

where one supposes that f is known at $N+1$ evenly spaced points in the range 0 to x with $f_N=f(0)$ and $f_0=f(x)$. Eq. (23) can be written in the form:

$$\frac{d^q f}{dx^q} = x^{-q} N^q \sum_{j=0}^{N} \varphi_j f_j \tag{24}$$

where:

$$\varphi_0 = \frac{1}{\Gamma(2-q)}[(n-1)^{1-q} - n^{1-q} + (1-q)n^{-q}]$$

$$\varphi_0 = \frac{1}{\Gamma(2-q)}$$

$$\varphi_{n-j} = \frac{1}{\Gamma(2-q)}[(j+1)^{1-q} - 2j^{1-q} + (j-1)^{1-q}] \quad 1 \le j \le n-1 \tag{25}$$

As regards the fractional oscillator, by assuming the displacement $u(t)$ $(0 \le t \le T)$ to be linear in each subinterval $[jh, (j+1)h]$ with $j=1, 2, \cdots, n$, from Eqs. (24) and (25) with $f(x)=u(t)$, Eq. (8) assumes the following form:

$$\frac{m}{h^2}(u_{n+1} - 2u_n + u_{n-1}) + \frac{c}{h^q} \sum_{j=0}^{n} \varphi_j u_j + k u_n = F(nh) \tag{26}$$

where the acceleration is expressed in accordance with the central difference algorithm. This equation leads to a linear system the unknowns of which are the displacement at the discrete time jh with $j=1, 2, \cdots, n$ (Koh and Kelly 1990). It should be noted that the coefficient matrix assumes a Gaussian form. The efficiency and the accuracy of the above integration procedure were tested with reference to single-degree-of-freedom (SDOF) base-excited by sinusoidal inputs. The maximum displacements and angle phases of its response evaluated by utilizing the numerical algorithm were compared to the results estimated by applying an analytical procedure in the frequency domain. Regarding this, it can be shown that a fractional derivative SDOF system is characterized by the following frequency response function (FRF):

$$H(f) = \frac{1}{K} \cdot \frac{1}{1 - \left(\frac{f}{f_0}\right)^2 + i^q \frac{c}{K}(2\pi f)^q} \tag{27}$$

where f_0 and f represent the natural frequency of the system and the frequency of the input action, respectively. Moreover, i^q is the q-order power of the imaginary unit:

$$i^q = \cos\left(\frac{\pi q}{2}\right) + i \sin\left(\frac{\pi q}{2}\right) \tag{28}$$

Several numerical tests were performed while varying f, f_0 and c; in Fig. 9, the comparison between the numerical and analytical $H(f)$ results referred to three c values are shown. A notable correspondence in all considered cases emerges.

6. Identification of parameters characterizing the *PD* device dynamic model

Preliminary numerical tests carried out in order to evaluate the dynamic response under sinusoidal inputs of fractional oscillators characterized by different q derivation order and damping

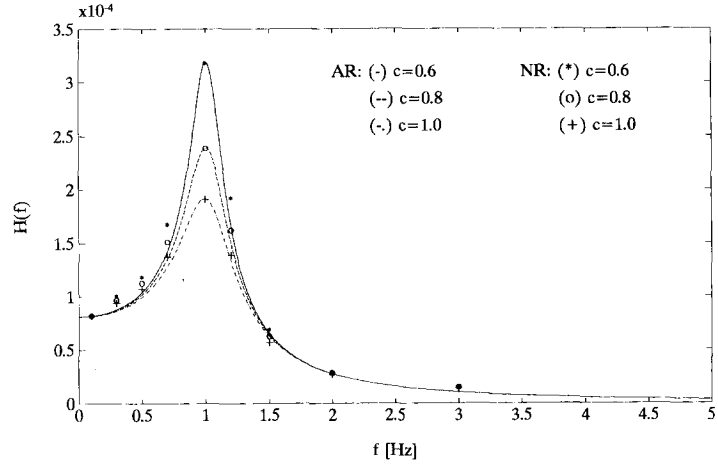

Fig. 9 Numerical (*NR*) and analytical (*AR*) $H(f)$ results referred to three c values (0.6, 0.8, 1.0 (kN/mm)s^q).

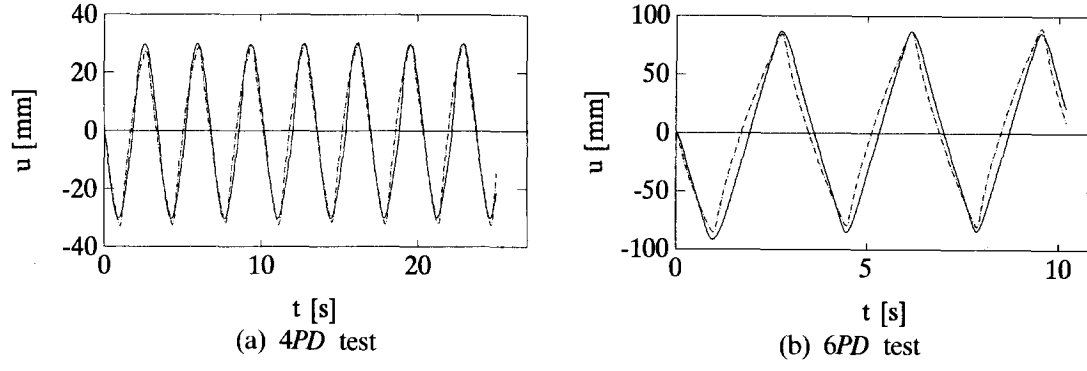

Fig. 10 Comparison between experimental (−) and numerical (−·−) displacement time histories.

coefficient c, pointed out that the displacement amplitude results are dependent on the q and c values, whereas the displacement phase depends only on q.

Based on these considerations, with reference to the *PD* device, the identification of the parameters characterizing the dynamic model was conducted by adopting the following criteria. By introducing in Eq. (26) without elastic term, the experimental force time history as input action $F(t)$, the identified q value is the one which permitted to obtain a displacement result on phase with respect to the corresponding time history experimentally imposed. In Fig. 10, a comparison between the experimental displacement functions relative to the 4*PD* and 6*PD* tests and the ones numerically obtained by assuming $q=0.8$ was presented. The q value identified in this case was verified to be the same for all the other test results relative to the *PD* device (Table 3). The damping coefficient was then calibrated by imposing that the experimental damping energy values should be equal to the numerical one. In Table 3, the estimated c values corresponding to each test are presented. With reference to the 4*PD* and 6*PD* tests in Fig. 11, a comparison between the experimental and the numerical hysteretical cycles is proposed. This figure outlines the good correspondence between the two results.

Table 3 *PD* device model: parameter values resulting from the identification procedure

	PD Device									
Test name	1*PD*	2*PD*	3*PD*	4*PD*	5*PD*	6*PD*	7*PD*	8*PD*	9*PD*	10*PD*
c(kN/mm)s^q	7.8	5.3	3.2	2.3	1.28	0.92	2.9	1.53	1.42	3.3
q	0.8	0.8	0.8	0.8	0.8	0.8	0.8	0.8	0.8	0.8

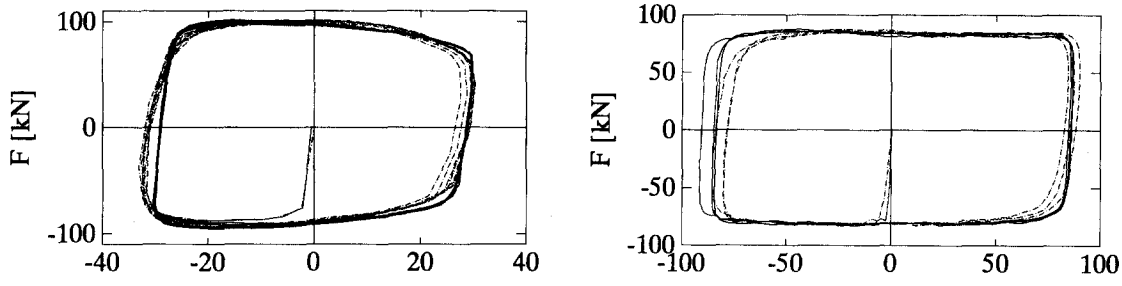

(a) 4*PD* test (b) 6*PD* test

Fig. 11 Comparison between experimental (−) and numerical (−·−) hysteretical loops.

Table 4 *ED* device model: parameter values resulting from the identification procedure

	ED Device								
Test name	1*ED*	2*ED*	3*ED*	4*ED*	5*ED*	6*ED*	7*ED*	8*ED*	9*ED*
c (kN/mm)s^q	2.2	2.7	1.2	1.0	0.72	0.78	0.8	0.3	0.23
q	0.9	0.9	0.9	0.9	0.9	0.9	0.9	0.9	0.9
k(kN/mm)	1.537	1.486	1.579	1.476	1.60	1.641	1.645	1.665	1.730

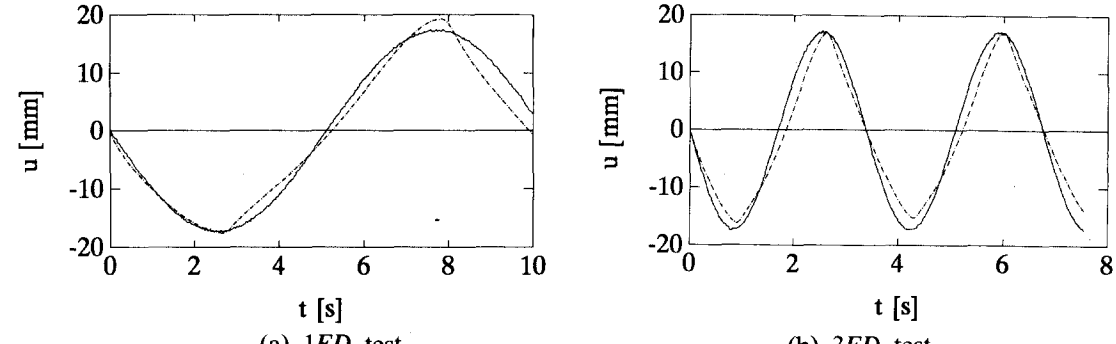

(a) 1*ED* test (b) 3*ED* test

Fig. 12 Comparison between experimental (−) and numerical (−·−) displacement time histories.

7. Identification of parameters characterizing the *ED* device dynamic model

With reference to the *ED* device, the identification of the q and c parameters was conducted

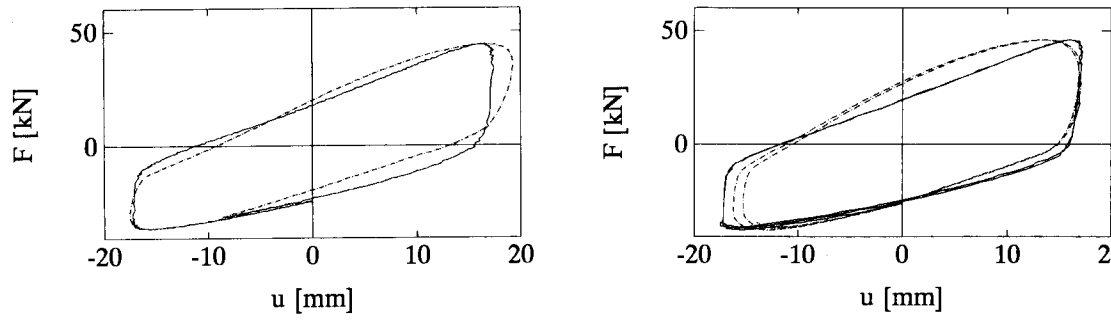

(a) 1*ED* test (b) 3*ED* test

Fig. 13 Comparison between experimental (−) and numerical (−·−) hysteretical loops.

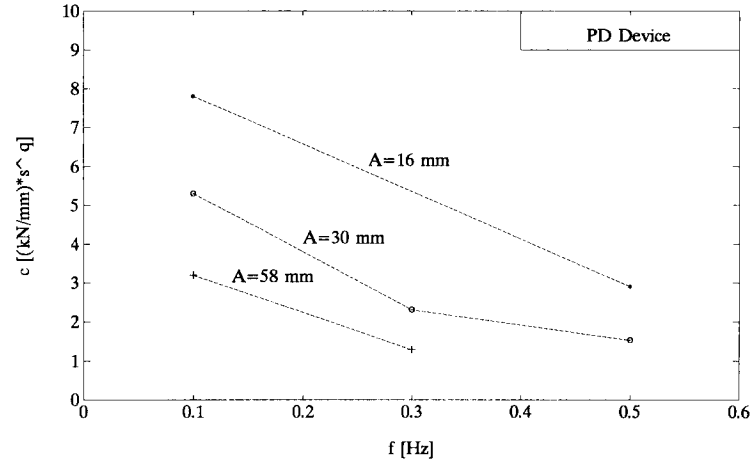

Fig. 14 *c-f* curves interpolating the results identified from three series of tests in which equal amplitude displacement time histories are imposed.

by applying the same criteria previously used for the *PD* system. In order to define the elastic component in Eq. (8), based on the experimental results a least square procedure permitted to evaluate a mean straight line with respect to each hysteretical cycle, the slope of which determines the k value for the linear model Eq. (6). In Table 4, the k, c and q identification results are presented. As shown, in general the scattering of every k value from their mean is less than 10%. With reference to the 1*ED* and 3*ED* tests, in Figs. 12-13 a comparison between the experimental results and the numerical ones is presented. As shown in these figures, the correspondence is acceptable also in the case of the elastic-damping model. With reference to the damping coefficient, the values indicated in Tables 3 and 4 show a variability of the c parameter depending on the frequency. This effect is evidenced also in Fig. 14, where three curves *c-f* are proposed. The interpolating curves there shown present the identification results obtained with respect to three series of tests carried out by imposing to the *PD* device sinusoidal displacement with different frequency f, but equal amplitude A.

8. Conclusions

In the paper, the mechanical behavior of a special typology of fluid viscous devices was modelled based on experimental test results and on a macroscopic rheological theory.

The results obtained by testing a pure damper as well as an elastic one showed that the behavior of the considered devices is characterized by a high mechanical and thermal stability. Moreover, the comparison between the hysteretical cycles of two systems pointed out the appropriateness of a Kelvin-Voigt scheme to interpret the superimposition of the elastic and the damping effects. By applying a fractional derivative model capable of reproducing the rheological behavior of polymeric materials such as the one contained in the tested devices, a fractional Kelvin-Voigt model was then proposed. The identification of the parameters characterizing the elastic and damping formulations (i.e., fractional derivative order, damping coefficient, and stiffness values) was carried out by means of a numerical algorithm purposely set-up. A comparison between the analytical and experimental results pointed out that the model is effective to interpret the dynamic behavior of the tested devices. However, from the identification phase emerged that the elastic element stiffness is frequency-independent, whereas the damping coefficient c is clearly dependent on frequency and on amplitude of the displacement time-history. Further studies concerning the theoretical modelling and the experimental as well as numerical analysis of the mechanical behavior of the devices for different frequency ranges will be carried out as future developments of the research.

References

Bird, R.B., Armstrong, R.C. and Hassager, O. (1987), *Dynamics of Polymeric Liquids,* John Wiley & Sons, New York.

Buckle, I.G. and Mayes, R.L. (1990), "Seismic isolation: history, application, and performance-A world view", *Earthquake Spectra,* **6**(2), 161-201.

Enelund, M. and Olsson, P. (1995), "Damping described by fading memory models", *Proc. 36th AIAA/ASME/ASCE/AHS/ASC Structures, Structural Dynamics and Materials Conf.,* New Orleans, LA, I, 207-220.

Huffman, G. (1985), "Full base isolation for earthquake protection by helical springs and viscodampers", *Nuclear Engineering and Design,* **84**, 331-338.

Kelly, J.M. (1993), *Earthquake-Resistant Design with Rubber,* Springer-Verlag, London.

Koh, C.G. and Kelly, J.M. (1990), "Application of fractional derivatives to seismic analysis of base isolated models", *Earthquake Engineering and Structural Dynamics,* **19**, 229-241.

Korenev, B.G. and Reznikov, L.M. (1993), *Dynamic Vibration Absorbers,* John Wiley & Sons, Chichester.

Makris, N. (1992), "Theoretical and experimental investigation of viscous dampers in applications of seismic and vibration isolation," Ph.D. Thesis, State University of New York, Buffalo.

Makris, N. and Constantinou, M.C. (1990), "Viscous dampers: testing, modelling and application in vibration and seismic isolation", *Technical Report NCEER-90-0028,* National Center for Earthquake Engineering Research, Buffalo, New York.

Nashif, A.D., Jones, D.I.G. and Henderson, J.P. (1985), *Vibration Damping,* John Wiley & Sons, Toronto.

Oldham, K.B. and Spanier, J. (1974), *The Fractional Calculus,* **111**, Academic Press.

Skinner, R.I., Robinson, W.H. and McVerry, G.H. (1993), *Seismic Isolation,* John Wiley & Sons, Chichester.

Terenzi, G. (1994), *Effetti Dissipativi nell Isolamento Sismico,* Ph.D. Thesis on Structural Engineering, University of Florence, Italy.